 

Plasma Sci. Technol. **19** (2017) 125303 (7pp) https://doi.org/10.1088/2058-6272/aa9027

# Altitude and intensity characteristics of parametric instability excited by an HF pump wave near the fifth electron harmonic

**Jun WU (吴军)[1], Jian WU (吴健)[1], M T RIETVELD[2,3], I HAGGSTROM[4], Haisheng ZHAO (赵海生)[1] and Zhengwen XU (许正文)[1]**

[1] National Key Laboratory of Electromagnetic Environment, China Research Institute of Radio Wave Propagation, Beijing 102206, People's Republic of China
[2] EISCAT , NO-9027 Ramfjordbotn, Norway
[3] UiT, The Arctic University of Norway, Tromsø, Norway
[4] EISCAT Scientific Association, Kiruna, Sweden

E-mail: wujun1969@163.com

Received 9 August 2017, revised 5 September 2017
Accepted for publication 26 September 2017
Published 25 October 2017


**Abstract**

An ionospheric heating experiment involving an O mode pump wave was carried out at European Incoherent Scatter Scientific Association site in Tromsø. The observation of the ultra high frequency radar illustrates the systematic variations of the enhanced ion line and plasma line in altitude and intensity as a function of the pump frequency. The analysis shows that those altitude variations are due to the thermal effect, and the intensity variations of the enhanced ion line are dependent on whether or not the enhanced ion acoustic wave satisfy the Bragg condition of radar. Moreover, a prediction that if the enhancement in electron temperature is suppressed, those systematic variations will be absent, is given.

Keywords: ionospheric heating, fifth harmonic, parameter instability, altitude, intensity

(Some figures may appear in colour only in the online journal)

## 1. Introduction

The parametric instability excited by the powerful radio wave has been studied extensively by Silin *et al* [1–14]. Based on some incoherent scatter radar measurements at Tromsø and Arecibo, the frequency spectrum including the enhanced plasma line and ion line as well as their asymmetries in intensity and width was studied [12, 15–21]. In order to excite the parametric decay instability (PDI) and oscillating two stream instability (OTSI), the pump has to exceed a threshold to overcome some saturation processes including the nonlinear Landau damping and the cascade type process for the lower pump power levels and the perturbations of the electron orbits by fluctuating fields for the higher pump levels [7, 22–24]. The dependence of the enhanced plasma line and ion line on the pump power indicates that they develop with increasing pump power [17, 21], and shows the 'hysteresis effect' for stepping up and down of the pump power [15]. In addition, PDI and OTSI are excited by the pump in O mode only, as is expected [15, 17]. The characteristic time of PDI and OTSI has been found to be on the order of microseconds [15–17, 20, 21, 25].

Due to the more complicated nature of the incoherent scatter spectrum obtained during Arecibo heating experiments, it had been seriously questioned whether the observations of ionospheric heating experiment can be explained in terms of PDI and OTSI. DuBois and his coworkers developed a new concept of strong Langmuir turbulence (SLT) and applied it to ionospheric modification experiment [26–28] and reported numerical and experimental results showing the coexisting of SLT with PDI [29, 30]. However, the experimental observations obtained at EISCAT show that PDI and OTSI represent the major process and the traveling Langmuir and ion acoustic waves the major features of incoherent backscatter spectrum [12].

The enhanced Langmuir wave and ion acoustic wave are excited by PDI and OTSI in the altitude range extending from the reflection altitude to approximately $0.1H$ km below the

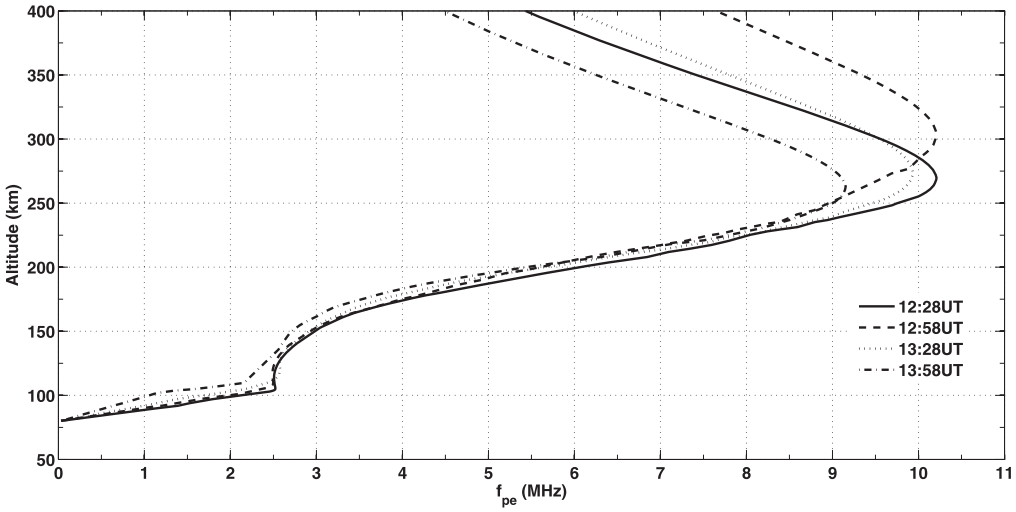


**Figure 1.** The altitude profiles of plasma frequency at EISCAT.

reflection altitude, where $H$ is the scale height of ionosphere plasma [12], and travel downward to be observed by the radar at the altitude where the radar Bragg condition is satisfied [12, 21, 31, 32]. Djuth *et al* [33] also presented some observations. An overshoot in plasma line intensity occurs when the HF beam is initially switched on. With increasing time the echo plunges downward by ∼3 km in altitude, exhibiting billowing, cloudlike structures in the range-time-intensity plot after ∼10 s of HF transmissions and reaching a bottom altitude after ∼25 s of HF transmissions; thereafter, a slight recovery toward greater altitudes is evident. Djuth *et al* [33] suggested that the above PDI plunges downward in altitude is most likely caused by changes in the electron density profile brought about by heating of the electron gas. Ashrafi *et al* [32, 34] observed a persistent pump induced enhancement in the ion line backscatter power near the HF reflection altitude, which started at ∼230 km and descended to ∼220 km within ∼60 s. The decrease in altitude of the ion line by ∼10 km and changes in electron density have been modeled.

The aim of this study is to understand the altitude and intensity characteristics of the enhanced ion line and plasma line by the pump near the fifth electron harmonic.

## 2. Experiment and observations

The EISCAT heater [35, 36] is located at Ramfjordmoen near Tromsø, Norway (69.58 °N, 19.21 °E, magnetic dip angle $I = 78°$). The 12 transmitters can generate up to ∼1.2 MW of continuous wave power in the frequency range from 3.85 to 8 MHz. There are three antenna arrays that cover the frequency ranges of 3.85–5.65 MHz and 5.5–8 MHz, two with a gain of ∼24 dB (dependent on frequency), which produce a beam width of 14.5° and a maximum effective radiated power (ERP) of ∼300 MW, and one with a gain of ∼30 dB resulting in a beam width of ∼7.5°. The principal diagnostic, EISCAT ultra high frequency (UHF) radar [37] located approximately 500 m from the EISCAT heater, is an incoherent scatter radar operating at 930 MHz. The antenna is a 32 m parabolic dish with a beam width of ∼0.5° at half-maximum power, and is fully steerable in azimuth and elevation.

A detailed description of the experimental arrangement have been given by Wu *et al* [38, 39]. To be more specific, the experiment was conducted at 12:30 UT–14:30 UT (universal time) on 11 March 2014. The EISCAT heater was operated in O mode at a frequency sweeping in steps of 2.804 kHz from 6.7 to 7 MHz near 5 $\Omega_{ce}$ as illustrated by the bottom panel of figures 2, 4 and 5, through which one can follow clearly the stepping change in pump frequency $f_{HF}$ and a modulation cycle of 18 min on, followed by 12 min off, where $\Omega_{ce}$ is the local electron cyclotron frequency at the altitude of ∼200 km in Tromso. The period of each step frequency sweep was 10 s. The heating beam was field-aligned (12.5° zenith, 186.2° azimuth), and ERP was estimated to be in the range 56–78 MW. The UHF radar started observations at 12:32:30 UT and remained field aligned with the 'beata' modulation. The 'beata' mode hass a 640 $\mu$s (32 × 20 $\mu$s) alternating code pulse with 10 $\mu$s sampling, which resulted in a decoded ∼2.5 km range resolution.

In addition, to measure the effect induced by the pump for each step of frequency, the data was analyzed by version 8.7 of Grand United Incoherent Scatter Design and Analysis Package (GUISDAP) software [40] and version 2.67 of real time graphic (RTG) using an integration time of 10 s.

The ionosphere was relatively quiet during the experiment. Figure 1 shows four altitude profiles of plasma frequency obtained through the measurement of the Dynasonde [41] at EISCAT at 12:28 UT, 12:58 UT, 13:28 UT and 13:58 UT respectively when the heater was off, and gives the reflection altitude difference of ∼3.5 km between 6.7 and 7 MHz. Besides, the local geomagnetic condition was relatively inactive, and the local electron gyrofrequency at the altitude of ∼200 km had a value of ∼1.366 MHz.

The 1st panel of figure 2 gives the altitude profile of radar echo $P$ with a height resolution of ∼2.5 km in the altitude range of 190–220 km. When the pump frequency $f_{HF}$ lies in the middle band, the radar echo $P$ is enhanced significantly

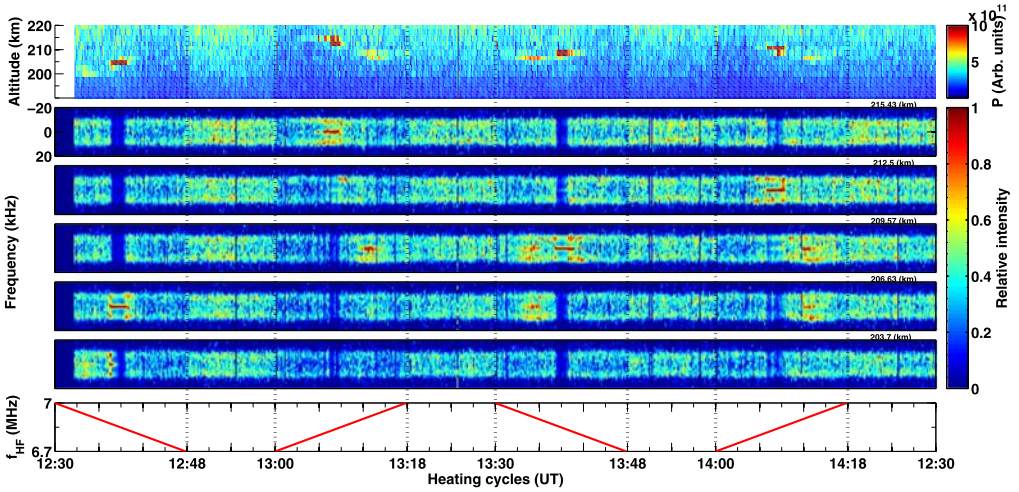


**Figure 2.** (1st panel) The power profile of UHF radar echo and (2nd–6th panels) ion line near the reflection altitude of the pump versus (7th panel) heating cycles.

near the reflection altitude of the pump. In the higher frequency band, the enhancements in $P$ are less than that in the middle band, the altitudes of which are lower than that in the middle band, not as expected from the electron density profile of the quiet ionosphere. When $f_{\rm HF}$ sweeps in the lower frequency band, $P$ is not enhanced. In order to facilitate the following description and discussion, it is necessary to divide the pump frequency band of [6.7 MHz, 7 MHz] into three bands, namely, the higher band (HB), the middle band (GB, close to the fifth harmonic) and the lower band (LB), where '[ ]' means the close interval. For instance the pump frequency can be divided into (6.857009 MHz, 7 MHz] as HB, [6.84299 MHz, 6.857 009 MHz] as GB and [6.7 MHz, 6.842 99 MHz) as LB respectively in the third cycle, where '( )' means the open interval. Indeed, due to the perturbation of the geomagnetic field, the above division in each cycle should be slightly different from each other.

In the 2nd–6th panels of figure 2, ion lines within the interval of [−20 kHz, 20 kHz] at altitudes of 215.43, 212.5, 209.57, 206.63 and 203.7 km are shown. It is necessary to point out that some gaps or weak ion line appearing in the GB are caused by the normalization of ion line at any particular time and altitude and do not imply any unusual response.

In the GB, some prominent enhancements in the ion line, the significant 'spikes' in the center manifesting OTSI and 'shoulders' at $\sim\pm$9.45 kHz confirming PDI [12, 21], are obvious around the reflection altitude. In the HB, however, these 'spikes' and 'shoulders' become weaker and are observed at a lower altitude than in the GB, which is not expected considering the altitude profile of the typical ionosphere. On the other hand, in the LB, there are not 'spikes' and 'shoulders' appearing at those altitudes. Those 'spikes' and 'shoulders' as well as their strength are coincident with the enhancements in $P$ temporally and spatially. Thus, we may draw safely a conclusion that PDI and OTSI induced by the pump lead to the enhancements in intensity of ion acoustic wave, furthermore, and to the enhancements in $P$ near the reflection altitude of the pump.

Previous observations at EISCAT showed that the altitude of the ion line was about 3–5 km higher than that of the plasma line [12, 21]. Indeed, this is always valid at EISCAT UHF radar, but it is difficult to explain the altitude difference between the enhanced ion line and plasma line. Stubbe *et al* [12] and Kohl *et al* [21] thought it was due to the virtual observation at a frequency 933 MHz/2. Therefore, the downshifted plasma lines within the frequency range from −6.7 to −7.25 MHz at altitudes of 198.52 km, 201.45 km, 204.39 km, 207.32 km, 210.25 km and 213.19 km respectively, are taken from the channel covering Doppler frequency offsets from −4.75 to −7.25 MHz and are shown in figure 3. It is clear that no enhanced plasma line occurs in the 1st panel of figure 3, namely, at the altitude of 213.19 km. This implies that the altitude of enhanced plasma line in the reported experiment follows the virtual observation at a frequency 933 MHz/2 given by Stubbe *et al* [12] and Kohl *et al* [21]. Similarly, these plasma lines show the weakening gaps caused by the normalization, but they occur in the GB and HB. At those altitudes, there are two 'layers' of plasma lines. The lower 'layer' of plasma lines lie at frequency $f_{\rm HF}$–$\omega_{\rm ia}$, as is expected as the 'decay line' from the PDI is excited by the pump, where $\omega_{\rm ia}$ is the frequency of ion acoustic wave with a value of $\sim$9.45 kHz. They show similar altitude features as the enhanced ion line, that is, the altitudes of the enhanced plasma lines in the HB are $\sim$3 km lower than that in the GB. Unlike the enhanced ion line, however, the intensity of the enhanced plasma lines in the HB does not become weak. The upper 'layer' of plasma lines are the spread of plasma lines at frequencies above the pump frequency and occur only at higher frequencies of ($\sim$6.93–7 MHz] in the HB. The nature of the upper 'layer' of plasma lines remains to be determined and exceeds the scope of this paper, but some possible explanations as the interaction of four plasma waves [42], the parallel traveling Langmuir waves generated by PDI scattering off the background lower hybrid density fluctuations [43, 44] and the free Langmuir wave excited by SLT [26–29], were proposed [39].

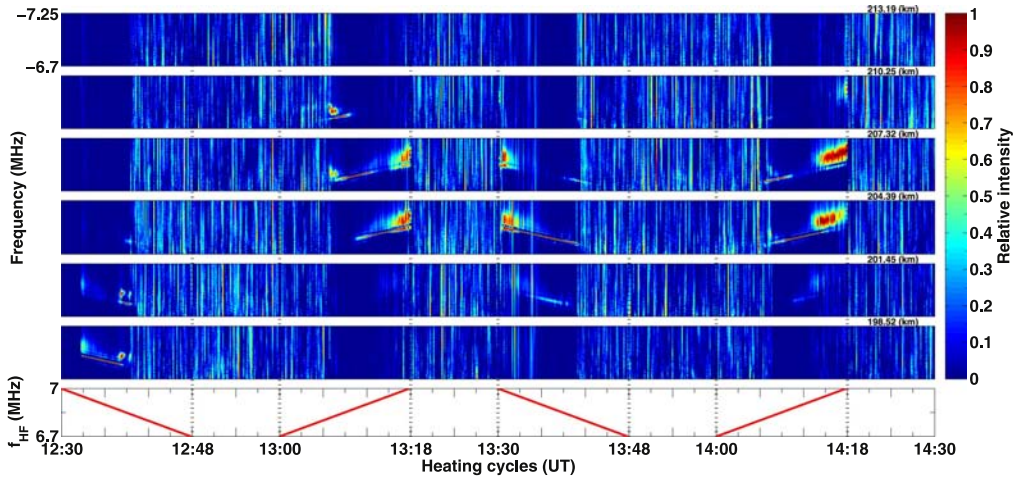


**Figure 3.** (1st–6th panels) The plasma line near the reflection altitude of the pump versus (7th panel) heating cycles.

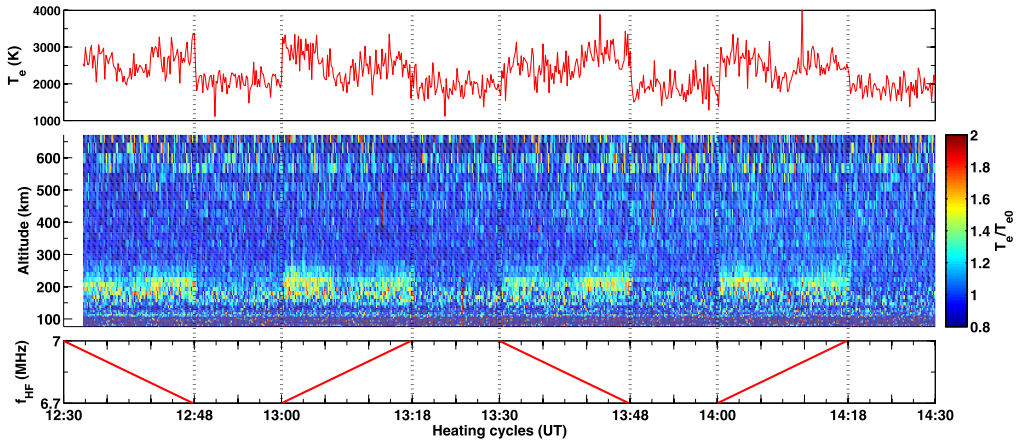


**Figure 4.** (1st panel) The electron temperature at altitude of ∼200 km and (2nd panel) the ratios of $T_e$ to $T_{e0}$ versus (3rd panel) heating cycles.

As an example, we give the electron temperature at altitude of ∼200 km in the 1st panel of figure 4, which shows that the electron temperature $T_e$ is ∼2000 K, ∼2100 K, ∼2500 K and 3000 K when the pump is off, and in the GB, HB and LB respectively. In addition, the 2nd panel of figure 4 gives the altitude profile of the ratios of $T_e$ to the undisturbed values of $T_{e0}$ as a function of heating cycle, where $T_{e0}$ was given by the median of the altitude profile of $T_e$ taken from the final 5 min of the last cycle. Those enhancements in $T_e/T_{e0}$ show the synchronization to the heating cycle and the variation with $f_{HF}$ in particular, namely, $(T_e/T_{e0})_{LB} > (T_e/T_{e0})_{HB} > (T_e/T_{e0})_{GB}$, where $(T_e/T_{e0})_{LB}$, $(T_e/T_{e0})_{HB}$ and $(T_e/T_{e0})_{GB}$ indicate $T_e/T_{e0}$ for the LB, HB and GB and have values of ∼1.5, ∼1.25 and ∼1.05 respectively. This dependents on the dispersion behavior of the electrostatic upper hybrid waves excited by an O mode pump at frequencies below, at and above the fifth electron harmonic respectively [39]. Actually, the systematic variety of the enhancement in $T_e$ induced by the pump near 5th gyroharmonic is similar to that near 3rd gyroharmonic. Fu *et al* [45] gave the evidence that when the pump frequency is near electron third gyroharmonic, the electron temperature enhancement measured by EISCAT-UHF radar is suppressed.

## 3. Discussion

Here we will no longer discuss such features of PDI and OTSI excited by the pump as the spectrum form, the characteristic time and the threshold, which have been described in detail by some authors mentioned in section 1, but only focus on those prominent features presented in section 2. In summary, (1) the altitude of the enhanced plasma lines and ion lines in the HB are ∼3 km lower than that in the GB, (2) the intensity of the enhanced ion lines in the HB is less than that in the GB, and (3) no enhanced plasma line and ion line were observed in the LB. As an example, the enhanced ion lines in the third heating cycle (13:30–14:00 UT) will be discussed in the following.

### *3.1. The altitude of the enhanced ion line*

The enhanced ion acoustic wave and Langmuir wave can be observed by a radar with frequency $f_r$ in monostatic operation at the altitude [12]

$$z = z_0 - 12\frac{K_B H f_r^2}{m_e c^2}\frac{T_e}{f_{HF}^2}, \quad (1)$$

where $z_0$ denotes the reflection altitude of the pump, $K_B$ the Boltzmann constant, $H$ the scale height with the reasonable

value of ~50 km at the altitude of ~200 km, $m_e$ the electron mass, $c$ the velocity of light and $f_{HF}$ the pump frequency. In this discussion, $z_0$ are assumed approximatively to be unchanged for the pump at frequencies [6.7 MHz, 7 MHz] by ignoring the tiny difference of 3.5 km between the reflection altitudes of the pump at frequencies [6.7 MHz, 7 MHz] shown in figure 1.

In the GB, due to the absence of the trapping of the upper hybrid wave in the small scale irregularity [39], $T_e$ enhances up to ~2100 K near the reflection altitude, then formula (1) can be expressed as $z_{GB} \approx (z_0 - 3.9)$ km, namely, 209.57 km. When the pump sweeps in the HB, however, the upper hybrid resonance can be converted into the fifth harmonic of Bernstein wave, further, which can be trapped in the small scale irregularity and result in the enhancement up to ~2500 K in $T_e$ around the reflection altitude [39], then formula (1) can be written as $z_{HB} \approx (z_0 - 4.65)$ km, which implies that the enhanced ion acoustic wave can be observed by radar at the slightly lower altitude than in the GB. Indeed, one can see in figure 2 that the enhanced ion lines in the HB occur at the altitudes of 209.57 and 206.63 km simultaneously, that is, the enhanced ion acoustic wave lies simultaneously in the range gates of 209.57 and 206.63 km. This should be reasonable by considering the radar height resolution of ~3 km.

Due to the higher heating rate induced by the trapping of the upper hybrid wave in the small scale irregularity and the lower cooling rate induced by the escape of thermal electron, the strongest enhancement of up to ~3000 K in $T_e$ occurs in the LB [39], formula (1) can be expressed as $z_{LB} \approx (z_0 - 5.58)$ km. Thus, the enhanced ion acoustic wave in the LB should have been observed by radar at the altitude 5.58 km below $z_0$, but the enhanced ion line was not present in figure 2, for which the responsible mechanism will be discussed in section 3.2.

On the other hand, the altitude decline of the enhanced ion line and plasma line is likely caused by changes in the electron density profile brought about by the heated ionospheric plasma [33]. Due to thermal electron transport, plasma may be pushed downward from the heating region, then the electron density profile may be changed. The 2nd panel of figure 4 shows that those enhancements in $T_e$ take place in the altitude range of ~180 to ~250 km, which implies that the electron density in the altitude range of ~180 to ~250 km may be suppressed, whereas the electron density below ~180 km will increase, then the reflection altitude of the pump may move downward and be at a particular altitude lower than ~180 km. However, figures 2 and 3 show that PDI and OTSI were excited in the altitude range from ~200 to ~220 km. Obviously, thermal electron transport could not change significantly the electron density profile in our case. Indeed, thermal conduction tends to smooth out the enhanced electron temperature profile, making significant plasma transport difficult to achieve and maintain over relatively small spatial scales [33]. Additionally, the plasma recombination rate being inversely proportional to electron temperature may allow the electron density profile to change. The increased electron temperature will decrease the dissociative recombination rate of molecular ions, especially in the lower portion of F region (below ~220 km) [46]. Thus the background electron density is expected to increase in response to the enhancement in electron temperature leading to a lowering of the reflection altitude of the pump.

Although we have focused on thermal effects of ionospheric heating on the altitude decline of the enhanced ion line and plasma line, we cannot clearly identify the dominant one of the above two mechanisms being responsible for the altitude decline of the enhanced ion line and plasma line. Additional experiments will be needed to examine the altitude of the enhanced ion line by (1) suppressing electron temperature and (2) modifying the reflection altitude of the pump, for instance above the altitude ~250 km, where fewer molecular ions are present.

### 3.2. The intensity of the enhanced ion line

With regard to the field aligned observation of radar in monostatic operation, the ion acoustic wave induced by PDI and OSTI follow reasonably the linear dispersion [47]

$$\omega_{ia}^2 = \gamma \frac{K_B}{m_i} T_e k^2, \tag{2}$$

where $\gamma$ is the adiabatic index, $m_i$ the ion mass and $k$ the wave number. When a wave is traveling in a non-uniform but stationary medium, its frequency will not change, but its wavelength changes. Indeed, figure 2 shows that the frequency of ion acoustic wave $f_{ia}$ $\left(\frac{\omega_{ia}}{2\pi}\right)$ keep unchanged and has a value of ~9.45 kHz. This implies that the term $T_e k^2$ in formula (2) will not change when the ion acoustic wave are traveling. In other words, with the constant $\gamma \frac{K_B}{m_i}$, $T_e$ and $k$ will be compensated by each other to keep $T_e k^2$ unchanged when the enhanced ion acoustic wave are traveling.

In figure 2, the EISCAT UHF radar observation in the third cycle shows that the strongest ion lines excited by OTSI and PDI occur in the GB and at the altitude of 209.57 km. It can then be identified approximately and reasonably that the wave number $k_{GB}$ of the enhanced ion acoustic wave satisfy the radar Bragg condition $k_{GB} = 2k_r$ exactly near the altitude of 209.57 km, where $k_r$ denotes the wave number of radar wave with a value of 19.6 $m^{-1}$ for the EISCAT UHF radar. In other words, a strong constructive interference of the enhanced ion acoustic wave traveling, is caused near the altitude of 209.57 km.

Considering $\omega_{ia}$ unchanged and the enhancement in $T_e$ of up to ~2500 K in the HB, the wave number of the enhanced ion acoustic wave $k_{HB}$ will become smaller than $k_{GB}$, that is, $k_{HB} = \sqrt{\frac{T_{eGB}}{T_{eHB}}} k_{GB} \approx 0.92 \times 2k_r$, which implies that $k_{HB}$ does not satisfy exactly the radar Bragg condition and a weaker constructive interference of the enhanced ion acoustic wave is caused, namely, the weaker ion lines observed in the HB, where $T_{eGB}$ and $T_{eHB}$ are the electron temperature around the reflection altitude in the GB and HB respectively.

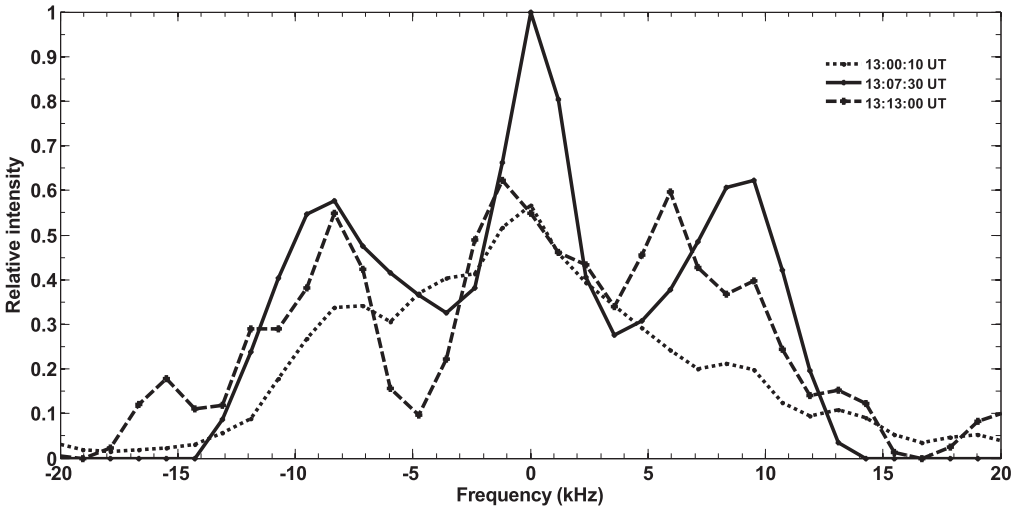


**Figure 5.** The enhanced ion lines at the altitude of 215.43 km at 13:00:10 UT, 13:07:30 UT and 13:13:00 UT.

In a similar way, the wave number of the enhanced ion acoustic wave in the LB $k_{\mathrm{LB}} = \sqrt{\frac{T_{\mathrm{eGB}}}{T_{\mathrm{eHB}}}} k_{\mathrm{GB}} \approx 0.84 \times 2k_{\mathrm{r}}$, can be obtained, which implies that $k_{\mathrm{LB}}$ does not satisfy remarkably the radar Bragg condition and leads to being unobserved by the UHF radar, where $T_{\mathrm{eLB}}$ is the electron temperature up to ~3000 K around the reflection altitude in the LB.

Obviously, in above case, $k_{\mathrm{LB}}$, $k_{\mathrm{GB}}$, and $k_{\mathrm{HB}}$ do depend only on $T_{\mathrm{e}}$. If the enhancement in $T_{\mathrm{e}}$ is suppressed as much as possible during ionospheric heating, the enhanced ion line and plasma line in the LB, GB and HB should have been observed by the UHF radar and shown with the same intensity. Likewise, a more detailed examination of this phenomenon is planned as part of future heating experiments at Tromsø.

As far as the variety of the intensity of the lower 'layer' of plasma lines is concerned, more work should be needed. Indeed, the enhanced Langmuir wave has the dispersion function and the propagating mechanism being different completely from that of ion acoustic wave.

Moreover, PDI and OTSI are excited regularly by the O mode pump in a few milliseconds [12, 21], thus the enhanced ion lines should be observed in the first data dump. However, one cannot see the enhanced ion line at 13:00:10 UT and 14:00:10 UT in figure 2. It should be emphasized here that the heating effect at 13:00:10 UT (and 14:00:10 UT) is induced by the pump starting at 13:00:00 UT (and 14:00:00 UT), when the corresponding pump frequency is 6.7 MHz. As an example, figure 5 shows three ion lines occurring at 13:00:10 UT (LB), 13:07:30 UT (GB) and 13:13:00 UT (LB) respectively, which are extracted from the 215.43 km panel of figure 2. One can see that the change in intensity of those ion lines is consistent with the above description in section 2. The most important is that the intensity of ion line in the first data dump (13:00:10 UT) is weak and does not confirm PDI and OTSI. This should be due to the characteristic time of PDI and $T_{\mathrm{e}}$. PDI and OTSI are excited in a few milliseconds [12, 21], and $T_{\mathrm{e}}$ is enhanced by the upper hybrid resonance within ~0.5 to ~5 s after the pump on [48], whereas the data was analyzed using an integration time of 10 s. Thus, it is clear that the disappearance of the enhancement in ion line in the first data dump (13:00:10 UT and 14:00:10 UT) is due to the long integration time of 10 s, which is depend on the sensitivity of radar.

## 4. Conclusions

This paper focuses on thermal effects of ionospheric heating on the altitude and intensity characteristics of the enhanced plasma line and ion line observed by EISCAT UHF radar during an ionospheric heating experiment performed on 11 March 2014 at EISCAT Tromsø site.

In conclusion, (1) the enhanced ion acoustic wave and Langmuir wave in the GB satisfy the radar Bragg condition and were observed by EISCAT UHF radar, as is expected, (2) due to the stronger enhancement in electron temperature in the HB than that in the GB, the enhanced ion acoustic wave and Langmuir wave were observed at a lower altitude in the HB than in the GB, (3) in the LB, the enhanced ion acoustic wave was not observed by radar, due to the strongest enhancement in electron temperature of ~3000 K, that is, PDI and OTSI were not absent in the LB, but were unobserved by EISCAT UHF radar due to the Bragg mismatching induced by the strong enhancements in electron temperature. It can be predicted that if the enhancement in electron temperature is suppressed, the enhanced ion acoustic wave and Langmuir wave in the LB may be observed by UHF radar, and the altitude decline of the enhanced ion line and plasma line in the HB will be absent, that is, the altitude of the enhanced ion line and plasma line in the HB will step upward with the increase in the pump frequency, as expected from the electron density profile of the quiet ionosphere.

## Acknowledgments

We would like to thank the engineers of EISCAT in Tromsø for keeping the facility in excellent working condition and Tromsø Geophysical Observatory, UiT The Arctic University of Norway, for providing the magnetic data of Tromsø recorded on 11 March 2014. The data from the UHF radar can be obtained freely from EISCAT (http://eiscat.se/schedule/schedule.cgi). The EISCAT Scientific Association is supported by China (China Research Institute of Radio Wave Propagation), Finland (Suomen Akatemia of Finland), Japan (the National Institute of Polar Research of Japan and Institute for Space-Earth Environmental Research at Nagoya University), Norway (Norges Forkningsrad of Norway), Sweden (the Swedish Research Council) and the UK (the Natural Environment Research Council).

## References

[1] Silin V P 1965 *Sov. Phys.—JETP* **21** 1127 (Engl. transl.)
[2] DuBois D F and Goldman M V 1965 *Phys. Rev. Lett.* **14** 544
[3] DuBois D F and Goldman M V 1967 *Phys. Rev.* **164** 207
[4] Perkins F W and Flick J 1971 *Phys. Fluids* **14** 2012
[5] Rosenbluth M N 1972 *Phys. Rev. Lett.* **29** 565
[6] Drake J F *et al* 1974 *Phys. Fluids* **17** 778
[7] Perkins F W, Oberman C and Valeo E J 1974 *J. Geophys. Res.* **79** 1478
[8] Kuo Y Y and Fejer J A 1972 *Phys. Rev. Lett.* **29** 1667
[9] Kuo S P and Cheo B R 1978 *Phys. Fluids* **21** 1753
[10] Chen H C and Fejer J A 1975 *Phys. Fluids* **18** 1809
[11] Fejer J A 1979 *Rev. Geophys.* **17** 135
[12] Stubbe P, Kohl H and Rietveld M T 1992 *J. Geophys. Res.* **97** 6285
[13] Wu J, Wu J and Xue Y 2006 *Int. J. Comput. Fluid Dyn.* **20** 491
[14] Wu J, Wu J and LaHoz C 2007 *Chin. Phys.* **16** 558
[15] Carlson H C, Gordon W E and Showen R L 1972 *J. Geophys. Res.* **77** 1242
[16] Gordon W E and Carlson H C 1974 *Radio Sci.* **9** 1041
[17] Kantor I J 1974 *J. Geophys. Res.* **79** 199
[18] Hagfors T *et al* 1983 *Radio Sci.* **18** 861
[19] Nordling J *et al* 1988 *Radio Sci.* **23** 809
[20] Stubbe P *et al* 1985 *J. Atmos. Terr. Phys.* **47** 1151
[21] Kohl H *et al* 1993 *J. Atmos. Terr. Phys.* **55** 601
[22] Bezzerides B and Weinstock J 1972 *Phys. Rev. Lett.* **28** 481
[23] Weinstock J and Bezzerides B 1972 *J. Geophys. Res.* **77** 761
[24] Dubois D F and Goldman M V 1972 *Phys. Fluids* **15** 919
[25] Jones T B *et al* 1986 *J. Atmos. Terr. Phys.* **48** 1027
[26] Dubois D F, Rose H and Russell D 1988 *Phys. Rev. Lett.* **61** 2209
[27] Dubois D F, Rose H and Russell D 1990 *J. Geophys. Res.* **95** 21221
[28] Dubois D F *et al* 1993 *J. Geophys. Res.* **98** 17543
[29] Dubois D F, Rose H and Russell D 1991 *Phys. Rev. Lett.* **66** 1970
[30] Djuth F T and Dubois D F 2015 *Earth Moon Planets* **116** 19
[31] Kohl H H *et al* 1987 *Radio Sci.* **22** 655
[32] Ashrafi M, Kosch M J and Honary F 2006 *Adv. Space Res.* **38** 2645
[33] Djuth F T *et al* 1994 *J. Geophys. Res.* **99** 333
[34] Ashrafi M *et al* 2007 *J. Geophys. Res.* **112** A05314
[35] Rietveld M T *et al* 1993 *J. Atmos. Terr. Phys.* **55** 577
[36] Rietveld M T *et al* 2016 *Radio Sci.* **51** 1533
[37] Rishbeth H A and Eyken V 1993 *J. Atmos. Terr. Phys.* **55** 525
[38] Wu J, Wu J and Xu Z 2016 *Plasma Sci. Technol.* **18** 890
[39] Wu J *et al* 2017 *J. Geophys. Res.* **122** 1277
[40] Lehtinen M and Huuskonen A 1996 *J. Atmos. Terr. Phys.* **58** 435
[41] Rietveld M T *et al* 2008 *Polar Sci.* **2** 55
[42] Borisova T D *et al* 2016 *Radiophys. Quantum Electron.* **58** 561
[43] Kuo S P and Lee M C 1992 *Geophys. Res. Lett.* **19** 249
[44] Kuo S P and Lee M C 1999 *Geophys. Res. Lett.* **26** 3289
[45] Fu H *et al* 2015 *Ann. Geophys.* **33** 983
[46] Kolesnik A G 1982 *Radiophys. Quantum Electron.* **25** 87 (Engl. transl.)
[47] Baumjohann W and Treumann R A 1996 *Basic Space Plasma Physics* (London: Imperial College Press) (https://doi.org/10.1142/p015)
[48] Gurevich A V 2007 *Phys.—Usp.* **50** 1091